

Comparing the viscoelastic properties of gelatin and different concentrations of kappa-carrageenan mixtures for additive manufacturing applications

Warner, E.I.; Norton, I.t.; Mills, T.b.

DOI:

[10.1016/j.jfoodeng.2018.10.033](https://doi.org/10.1016/j.jfoodeng.2018.10.033)

License:

Creative Commons: Attribution-NonCommercial-NoDerivs (CC BY-NC-ND)

Document Version

Peer reviewed version

Citation for published version (Harvard):

Warner, EL, Norton, IT & Mills, TB 2019, 'Comparing the viscoelastic properties of gelatin and different concentrations of kappa-carrageenan mixtures for additive manufacturing applications', *Journal of Food Engineering*, vol. 246, pp. 58-66. <https://doi.org/10.1016/j.jfoodeng.2018.10.033>

[Link to publication on Research at Birmingham portal](#)

Publisher Rights Statement:

Checked for eligibility 04/01/2019

<https://doi.org/10.1016/j.jfoodeng.2018.10.033>

General rights

Unless a licence is specified above, all rights (including copyright and moral rights) in this document are retained by the authors and/or the copyright holders. The express permission of the copyright holder must be obtained for any use of this material other than for purposes permitted by law.

- Users may freely distribute the URL that is used to identify this publication.
- Users may download and/or print one copy of the publication from the University of Birmingham research portal for the purpose of private study or non-commercial research.
- User may use extracts from the document in line with the concept of 'fair dealing' under the Copyright, Designs and Patents Act 1988 (?)
- Users may not further distribute the material nor use it for the purposes of commercial gain.

Where a licence is displayed above, please note the terms and conditions of the licence govern your use of this document.

When citing, please reference the published version.

Take down policy

While the University of Birmingham exercises care and attention in making items available there are rare occasions when an item has been uploaded in error or has been deemed to be commercially or otherwise sensitive.

If you believe that this is the case for this document, please contact UBIRA@lists.bham.ac.uk providing details and we will remove access to the work immediately and investigate.

1 Comparing the viscoelastic properties of gelatin and different 2 concentrations of kappa-carrageenan mixtures for additive 3 manufacturing applications

4 E. L. Warner*, I. T. Norton and T. B. Mills

5
6 School of Chemical Engineering, University of Birmingham, Edgbaston, B15 2TT, UK

7 *Corresponding author. E-mail address: ELW198@bham.ac.uk

8 9 Abstract

10 Recent interest in personalisation of food through additive manufacturing has
11 identified a need for more information on the formulation and printability of potential
12 ingredients. The printability of four different mixtures of two food hydrocolloids, gelatin
13 and kappa-carrageenan were investigated. Design rules were established to
14 determine whether the materials fit the requirements of the process. The gelling
15 temperatures of the systems and the rheological characteristics including: flow
16 profiles, evolution of elastically dominated structures and frequency dependent
17 behavior were established. The mixtures were subsequently printed at two
18 temperatures, just above and much greater than, the gelling temperatures. Analysis
19 showed the rheological behaviours accompanying the coil-helix transitions of the
20 systems were key to printing the product in a well-defined manner. Printing fidelity was
21 related to the changes in elastic modulus, where rapid formation of an elastic network
22 gave rise to defined shapes with the ability to self-support under multiple layers.

23 24 Keywords

25 Additive manufacturing; gelatin, kappa-carrageenan; microstructure; rheology;
26 printability.

27 28 1. Introduction

29 The use of additive manufacturing to be able to design and control the microstructure
30 within food products has a huge potential for impact on the food industry. It would
31 enable the production of foods with detailed ingredient distribution, resulting in highly
32 efficient use of materials (Diaz et al., 2014). Additionally, additively manufacturing food
33 could also lead to the formulation of products with predefined textural and release
34 properties, tailored to the individual consumer's requirements. Although in theory
35 ideal, the incorporation of this technique into everyday use still has many challenges.

36 One of the most prominent being incorporation of products into the consumer supply
37 chain: requiring the widespread design of printers and formulations capable of printing
38 numerous products. For this reason, much effort is going into understanding the
39 design principles required for printing food products with the aim to translate them into
40 the additive manufacturing field.

41

42 The term “additive manufacturing” encompasses many different techniques, whereby,
43 an object is created through the deposition of materials layer by layer (Godoi et al.,
44 2016). Whilst additive manufacturing techniques such as selective laser sintering
45 (SLS) have been used for the production of food products (Diaz et al., 2016), the main
46 focus of the researched is based on fused deposition modelling (FDM). FDM uses an
47 extrusion/deposition process in order to create 3-dimensional objects. This technique
48 was originally created for use with thermoplastic materials in filament form (Wohlers
49 and Gornet, 2012), worked by motors pulling solid filament into a nozzle where heat
50 is applied to melt the material to create a flowable, fluid state (Crump, 1992). The
51 material is then extruded and deposited onto the build platform, where cooling leads
52 to solidification (Kruth et al., 1998).

53

54 FDM has been slow to move into the food industry, as the complex nature of foods
55 pose many challenges: multi-component, controlled microstructures for sensory
56 attributes, multiple thermal transitions and polymorphs *etc.* For this reason, there is
57 limited literature on the thermal printing of food products, with most of the examples
58 focused around the thermal extrusion of chocolate (Hao et al., 2010). However, a
59 much wider range of materials are required if FDM is going to become a commercially
60 viable option. As such, much of the current research has been focused on the printing
61 of materials through extrusion that are intrinsically thixotropic at room temperature;
62 providing a means of flowing through the nozzle and thickening again without the need
63 of thermal transitions. Cohen et al. (2009) has demonstrated the use of a syringe
64 based FDM process to print combinations of low concentration gelatin and xanthan
65 gum. It was shown that it was possible to simulate a wide variety of mouth feels,
66 ranging from systems with sensory attributes for chocolate through to risotto by using
67 these two ingredients. Yang et al. (2018) developed an FDM machine to determine
68 the optimum printing parameters for the printing of lemon juice gel. To ensure that the
69 desired geometry was achieved from the printed shape, Yang and his team

70 investigated different printing parameters, including nozzle height, diameter and
71 movement speed in order to determine their optimum values. These parameters were
72 assessed by printing lines and cylinders while varying the parameters and then visually
73 observing which had printed closest to the target geometry. They determined that a
74 storage modulus (G') of ca. 5 kPa, nozzle height and diameter of 1 mm and a nozzle
75 moving speed of 30 mm/s enabled the printing of the most precise shapes. Although
76 such materials have demonstrated much promise in the field, they are often
77 impractical, being too weak to mechanically manipulate preventing them from being
78 moved/packaged *etc.* One answer to this are thermo-reversible hydrogels, using a
79 thermal process to structure the materials with controlled mechanical properties.

80

81 Gelatin and kappa-carrageenan (κ C) are both thermo-reversible polysaccharides
82 commonly used within the food industry. Gelatin is obtained by the partial hydrolysis
83 of collagen, which is derived from animal skin and bones; it is favoured by
84 manufacturers because its body-temperature melting point produces a desirable
85 mouthfeel (Morrison et al., 1999). The gelation of gelatin occurs through the transition
86 of random coils into helices and gels as the temperature is decreased (Joly-Duhamel
87 et al., 2002). κ C originates from a family of linear polysaccharides extracted from
88 different species of red algae (Mangione et al., 2005). Gelation of κ C has been
89 attributed to the double helix formation which involved regular sequences between the
90 kink point on two adjacent chains (Rees, 1972). Upon the addition of κ C to gelatin,
91 there occurred an interaction between the positively charged amine groups within the
92 gelatin and the negatively charged sulfate groups within the κ C (Antonov and
93 Gonçalves, 1999). This led to the formation of (bio)polyelectrolyte complexes, which
94 affected the thermo-stability of the system, increasing the gelation rate (Derkach et al.,
95 2015). The formulation of gelatin alone was a transparent mixture, but upon addition
96 of κ C, the mixtures became turbid. This was due to associative phase separation of
97 the two polymers (Antonov and Gonçalves, 1999).

98

99 The properties of the materials to be extruded within the FDM process play a key part
100 in determining whether the material will be printable. Some research has already been
101 undertaken in order to investigate how the rheological properties of different materials
102 affect their printability. Liu et al. (2017) investigated the printability of mashed potato

103 modified with various amounts of potato starch by researching the viscosity and
104 viscoelastic properties. It was established that the ideal addition of potato starch was
105 2%, exhibiting a yield stress of 312.16 Pa and a G' of around 4 kPa. Lower amounts
106 of potato starch produced lower yield stress and the printed objects sagged; the
107 addition of more potato starch led to difficulty in extruding due to the resultant high
108 value of the consistency index (214.27 Pa.sⁿ). Li et al. (2016) also explored the use
109 of biopolymers, alginate-based hydrogels, in an effort to quantify the quality of 3D
110 prints at ambient temperatures. Here they determined that the thixotropic nature of the
111 gel was key to good printability, a property that could be finely tuned through the
112 addition of graphene oxide, to allow them to manipulate the uniformity of the printed
113 shape.

114

115 Research undertaken to date has concentrated on exploring the rheological properties
116 and printability of hydrogels using materials which maintain their shape due to a yield
117 stress. Whilst this technique is satisfactory, a greater variety of foods and finishes
118 could be provided with the benefit of an enhanced understanding of the material
119 properties necessary in order to print food that transitions from a liquid to a solid.

120

121 The main objectives of this study were, therefore, to investigate the viscoelastic
122 properties of a temperature dependent gelatin-based solution and then correlate these
123 properties with the printability of the material.

124

125 2. Materials and methods

126 2.1. Materials

127 Porcine gelatin (250 bloom), and κ C were purchased from Sigma-Aldrich (UK).
128 Reverse osmosis water was used, which had been purified using a millipore purifier.
129 The materials were used without any further purification or modifications.

130

131 2.2. Preparation of the gelatin and κ C solutions

132 Four different formulations were investigated, 5% gelatin with 0, 1, 2 and 3% κ C. The
133 samples were prepared by dispersing the required amount of κ C into the reverse
134 osmosis water at a temperature of 70°C on a heated bed, under agitation using a
135 magnetic stirrer bar for 30 minutes. Subsequently, the gelatin was added to the

136 solution, at a temperature of 60°C, and left to fully hydrate for 30 minutes in
137 correspondence with (Takayanagi et al., 2000), under agitation.

138

139 2.3. Characterisation of the formulations

140 2.3.1. μ DSC

141 A Seteram MicroDSC 3 evo (Seteram, France) was used to analyse the thermal
142 transitions of the formulations. 0.67 g \pm 0.06 g of a gelatin mixture was packed into the
143 stainless-steel cell. The reference cell was filled with an equivalent amount of reverse
144 osmosis water. Samples were then analysed using the following profile: initially the
145 sample was cooled to a temperature of 0°C and then held there for 60 minutes. A
146 heating ramp was applied at a scanning rate of 1.2°C/min up to 60°C and then cooled
147 at the same rate back to 0°C, where it was held for another 60 minutes. This cycle
148 was repeated twice, so that 3 heating and 3 cooling curves were obtained in total. The
149 maximum temperature of 60°C was used as all the transitions were complete within
150 this temperature range (Iijima et al., 2007, Wang et al., 2015). Gelling temperatures
151 were determined as the onset of the exothermic peak.

152

153 2.3.2. Rheological measurements

154 Rheological measurements were performed on a Kinexus pro rheometer (Malvern,
155 UK). Three different tests were undertaken: (1) single frequency, (2) frequency
156 sweeps and (3) a custom-made profile to mimic the extrusion process.

157

158 *Oscillation test at a single frequency*

159 An oscillation test undertaken at a single frequency was conducted at a frequency of
160 1 Hz and a strain of 1%. The sample was loaded at 60°C and cooled at a rate of
161 1°C/min to 20°C, during which the evolution of the G' and loss modulus (G'') were
162 recorded. A serrated 60mm parallel plate geometry was used, with a gap of 1mm for
163 the formulations with κ C, and a gap of 0.35 mm for the formulation without κ C. This
164 geometry was used in order to avoid slip and a small amount of silicon oil was spread
165 around the lip of the geometry, to act as an oil trap in order to prevent evaporation of
166 the mixture.

167

168 *Frequency sweep*

169 Frequency sweeps were obtained for all the samples measuring the G' and G'' through
170 a range of applied frequency (0.1-10 Hz). This range was within the linear viscoelastic
171 region of all materials, as determined by amplitude sweeps (data not shown). The tests
172 were undertaken at 20, 30, 40 and 50°C, apart from the 5% gelatin formulation, which
173 was only tested up to 40°C, due to the sensitivity of the rheometer. A serrated plate
174 was used with a gap of 0.35mm at temperatures above the gelling temperatures of
175 each of the materials and a gap of 1mm at temperatures tested below the gelling
176 temperatures. The only exception was the 5% gelatin, where a gap of 0.35mm was
177 used for all measurements, due to its low viscosity.

178
179 *Custom-made profile to mimic the extrusion process*

180 A custom-made extrusion sequence was run in order to simulate how the material
181 would behave as it passed through the nozzle and post-extrusion. When the material
182 passes through the nozzle, it will experience a shearing force and a temperature drop.
183 Both of these variables will affect how the material will flow, therefore it was important
184 to investigate how they affected the material's behaviour. Once the material was
185 extruded, it needed to have a fast recovery rate, in order for it not to spread and also
186 be able to support the weight of any subsequent layers. A two-part sequence was
187 created; the first part investigated how the viscosity of the material was affected
188 through a range of temperatures. The temperature range was reduced from 40°C-20°C
189 for the 5% gelatin only and from 50°C - 20°C for the gelatin with κC mixtures. A lower
190 temperature range was used for the formulation with just gelatin, as the properties of
191 this mixture at higher temperatures were outside the sensitivity of the rheometer used.
192 The average shear rate within the nozzle was determined using equation 1.

193
$$\dot{\gamma} = \frac{4Q}{\pi R^3} \quad [1]$$

194
195 *Where $\dot{\gamma}$ is the shear rate, Q is the flow rate and R is the radius of the nozzle.*

196
197 Initially, the flow rate was found by printing a shape of known volume (10.26 ml) and
198 recording the time taken to print. The flow rate was then determined using equation 2.

199
$$Q = \frac{V}{t} \quad [2]$$

200

201 *Where V is the volume of the printed part and t is the time.*

202

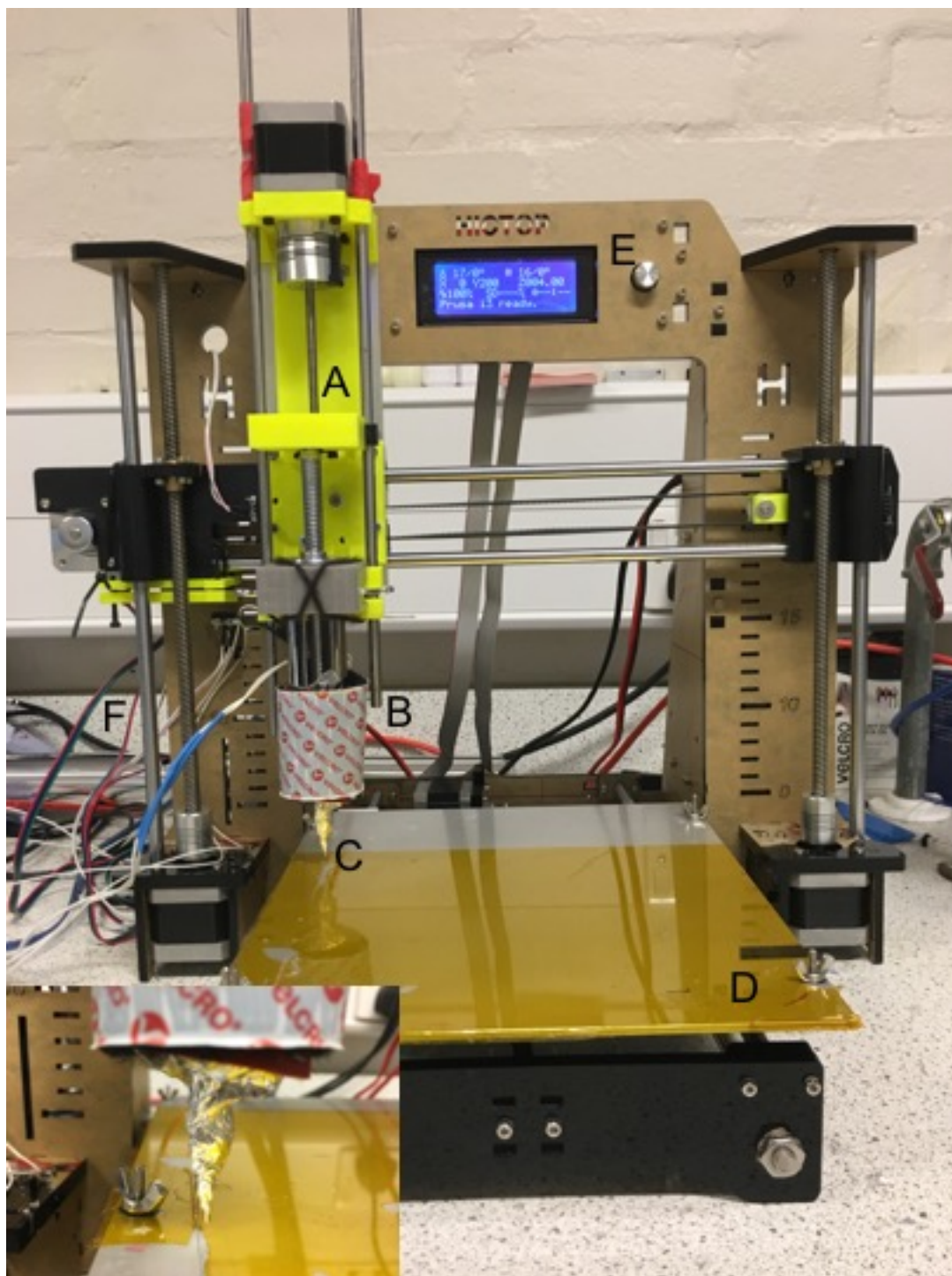
203 The shear rate applied to the material during extrusion through the syringe barrel
204 (needle) was calculated to be of the order of 100 s^{-1} , closely corresponding to previous
205 data presented by Li et al. (2016). The second part of the sequence measured the G'
206 and G'' over 10 minutes at a frequency of 1Hz and strain of 0.1%. A serrated plate
207 geometry was used for all these tests, with a gap of 1 mm.

208

209 2.4. Creation and use of the syringe pump printer

210 The custom-made FDM printer was created by modifying a commercially available
211 Hictop Prusa i3 printer. Firstly, the original nozzle was replaced with a 30 ml metal
212 syringe and a back plate which was designed and printed in plastic. The syringe was
213 encased in a silicone heater pad and controlled using a stepper motor connected to a
214 screw plunger. A metal needle of 0.6 mm diameter, purchased from TECHCON
215 (Hampshire, UK) was used. During the printing process, the syringe was loaded with
216 approximately 15 ml of material (due to the height of the heater pad only covering this
217 much of the syringe) and then the needle was attached and insulated using aluminium
218 foil in order to prevent temperature loss. The syringe was attached to the back plate
219 and held there using printed clasps during the printing process. Figure 1 shows a
220 labelled picture of the syringe printer, with the insert showing a close-up of the
221 insulated needle.

222



224

225 *Figure 1. Labelled photograph of the Hictop Prusa i3 printer, with the custom syringe pump (A. Custom built back plate, B.*
 226 *Metal syringe encased in a silicone heating pad, C. Metal needle insulated with tin foil, D. Printing bed, E. Control display, F.*
 227 *Circuit board that connects to the printer and controls the motors). Insert shows a close-up of the insulated needle.*

228

229 The software used to control the printer was 'Repetier'. In order to create the object, a
 230 computer-aided design (CAD) model of the object was inputted into the software
 231 (Wong and Hernandez, 2012). The software then 'slices' the object into layers and

232 calculates a path that is then used for the creation of the object. During the printing
233 process, the syringe followed this path and extruded material where necessary, in
234 order to create the shape.

235

236 Before each print the bed level was calibrated manually at the four corners of the bed
237 by using a 100 micron gauge. In all cases, systems were printed at ambient
238 temperatures without the aid of external cooling apparatus. During the prints, the
239 printing speed was set to 10 mm/s and the non-print moving speed was set to 100
240 mm/s. The layer height of the objects was maintained at 0.3 mm for all of the layers.

241

242 2.5. Statistical analysis

243 All of the μ DSC and rheological experiments have been repeated in triplicate, while
244 the printed squares have been repeated 6 times. All of the data has been presented
245 as the mean of the results \pm 1 standard deviation. Data analysis of the width and the
246 heights of the printed squares was processed with SigmaPlot software, with
247 differences of $p < 0.05$ considered to be significant.

248

249 3. Results and discussion

250 Initially, within this project, mixtures of just gelatin were investigated for the extrusion
251 process, because of their high gel strength (Gómez-Guillén et al., 2011). However,
252 conversion of the coils to helices in gelatin is a slow process (Harrington and Morris,
253 2009), which meant that the printed objects did not retain their shape after printing. κ C
254 was added in order to accelerate the gelation of the system enabling better shape
255 retention.

256

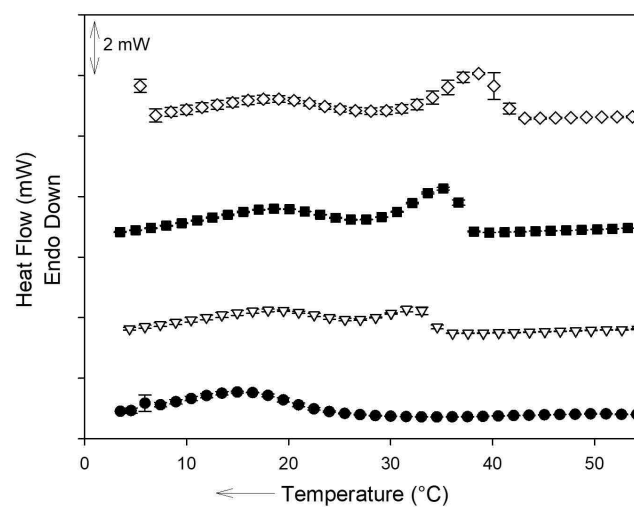
257 3.1. Thermal properties of the gelatin and κ C mixtures

258 The behaviour of the material within the nozzle will be affected by its thermal
259 properties. such properties of the various printing materials (5% gelatin and 0, 1, 2 and
260 3% κ C) were investigated using a μ DSC and rheological techniques.

261

262 Figure 2 demonstrates the first cooling cycles, from 60°C to 0°C, for 5% gelatin with
263 additions of 0, 1, 2 and 3% κ C, found from the μ DSC. The 5% gelatin exhibits a single
264 exothermic peak which was attributable to the coil-helix transformation of the gelatin
265 (Michon et al., 1997). The result determined for the 5% gelatin was found to be

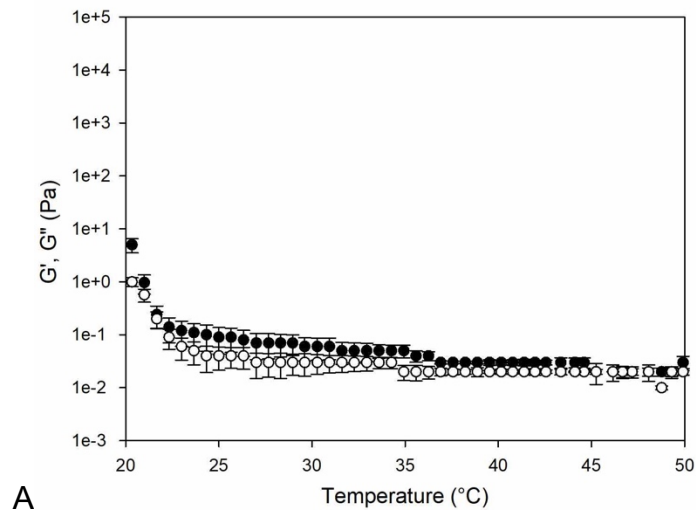
266 comparable to the result found by Bohidar and Jena (1993). Following the addition of
267 the various concentrations of the secondary bio-polymer, κ C, two exothermic peaks
268 were observed on each of their respective μ DSC curves. The broad peak spanning
269 10 to 20 °C was attributed to the gelation of the gelatin. The second peak at much
270 higher temperatures, ca. 30 °C, was attributable to the gelation of the κ C as also
271 observed by Wang et al. (2015). The results obtained for the κ C were found to be
272 similar to be similar to results obtained by Iijima et al. (2007), who looked at different
273 concentrations of κ C.
274



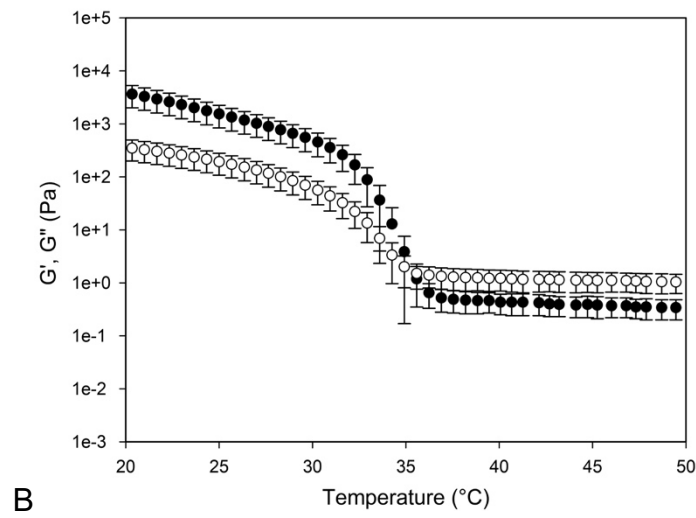
275
276 *Figure 2. μ DSC curves of 5% gelatin with 0% κ C (●), 1% κ C (▽), 2% κ C (■), and 3% (◇). ($n=3 \pm SD$).*

277
278 The gelation of the two bio-polymers was further explored using a rotational
279 rheometer. The oscillation test at a single frequency sweep was run from a
280 temperature of 60 °C to 20 °C and the results for the G' and G'' for 5% gelatin mixtures
281 with the addition of 0, 1, 2 and 3% κ C are shown in Figures 3 A, B, C and D
282 respectively.

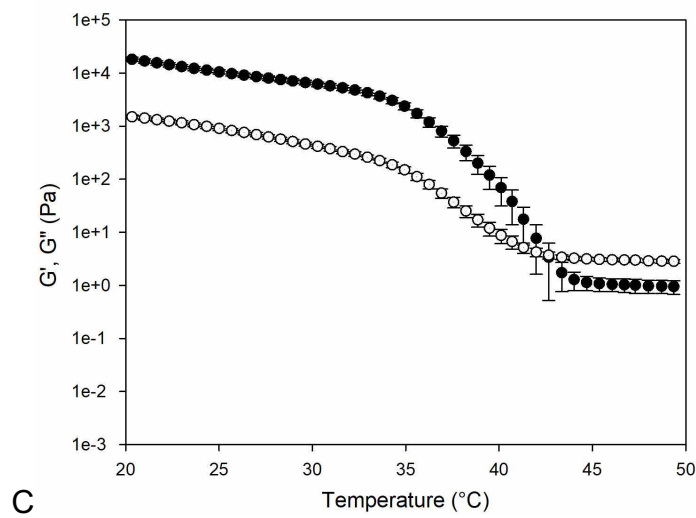
283

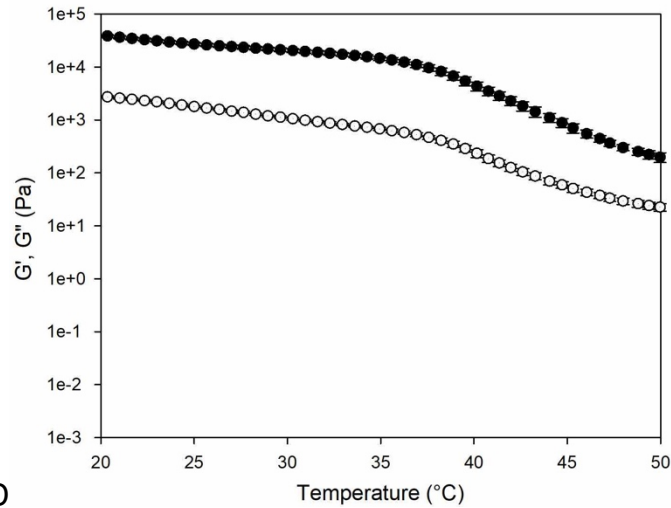


284



285





286

D

287 *Figure 3. Figure 3. G' (●) and G'' (○) of 5% gelatin and 0% κC (A), 1% κC (B), 2% κC (C) and 3% (D). (n=3 ± SD).*

288

289 G'' was greater than G', at high temperatures for all of the formulations, with the
 290 exception of 5% gelatin and 3% κC. This result indicated that at high temperatures the
 291 systems behaved as a viscoelastic liquid. At 24, 36 and 44 °C for the formulations with
 292 0, 1 and 2% κC respectively, there was a rapid increase in both G' and G''. This
 293 increase would appear to be due to the random coils (initially of the κC, and then the
 294 gelatin) within the mixture transitioning to ordered helices through hydrogen bonding
 295 (Parker and Povey, 2012). A cross-over point occurred between G' and G'' shortly after
 296 the increase and the temperature this happened was taken as the gelling temperature
 297 in accordance with Djabourov et al. (1988). Results obtained for the 5% gelatin
 298 solution, using this method, was similar to that obtained by Tosh and Marangoni
 299 (2004), who determined the gelling temperature to be 24.5 °C. The slightly higher
 300 temperature found by Tosh and Marangoni could be attributed to the slower rate and
 301 higher frequency that they used.

302

303 At temperatures lower than the gelling temperature, the G' was greater than the G''.
 304 This indicated that the mixture behaved as a viscoelastic solid, likely owing to the
 305 rheologically significant sample-spanning network of polymeric helices. The
 306 formulation with 3% κC displayed a higher G' across the whole range of temperatures
 307 tested, indicating that, even at high temperatures, such a high concentration of
 308 polymer within the solution resulted in the material being elastically dominated.

309

310 The results from both the μ DSC and the rheological data indicated that the addition of
311 additional κ C resulted in a higher temperature being required for gelling (table 1).

312

313 As the temperature was reduced below the gelling point of the κ C, gelation of the κ C
314 commenced, forming an elastic self-supporting structure which acted as a scaffold for
315 the gelatin. When the temperature was subsequently reduced to the gelling point of
316 the gelatin, gelation of the gelatin commenced leading to further solidification and
317 strengthening of the hydrogel. The control of the printability of the material and the
318 resultant resolution of the product could be enhanced by this two-step mechanism as
319 it would prevent the primary polymer (gelatin) from spreading during the cooling
320 process.

321

322 The gelling temperatures obtained from both the rheometer and the μ DSC were found
323 to be very similar. The small difference observed may have been due to the different
324 rates used for each of the pieces of equipment. The results found from the onset of
325 the μ DSC were taken forward as the gelling temperature.

326

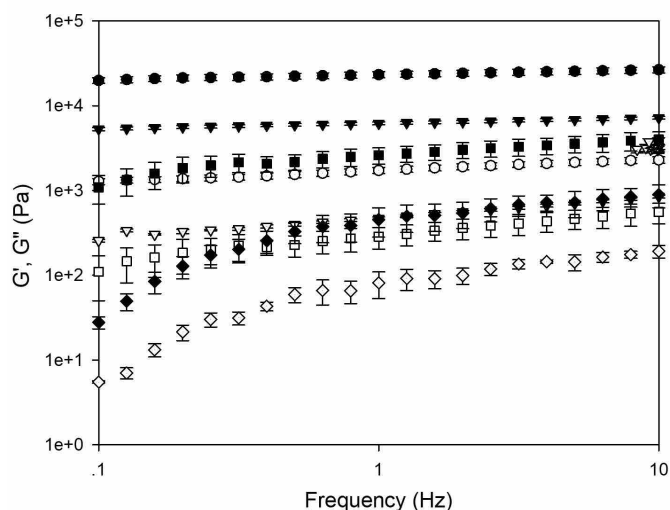
327 3.2. Rheological characterisation of the gelatin mixtures

328 It is important to understand the rheological properties of the materials to be printed
329 because the resultant product must not only be edible but it must also be desirable.
330 (Van Vliet, 2013).

331

332 Frequency sweeps were performed on all of the materials at different temperatures,
333 both above and below their gelling temperature. The G' and G'' determined from the
334 frequency curves obtained from a mixture of 5% gelatin and 2% κ C at 20, 30, 40 and
335 50°C can be seen in Figure 4. The shape of the curves obtained were typical for all of
336 the other formulations.

337



338

339 *Figure 4. Frequency Sweeps of 5% Gelatin and 2% κC at 20°C (○), 30°C (▽), 40°C (□) and 50°C (◇), open symbols are the*
 340 *G'', while closed symbols are the G'. (n=3 ± SD).*

341

342 For each of the different materials tested, when the testing temperature was greater
 343 than the gelling temperature, both G' and G'' were dependent on frequency; this
 344 demonstrated that the materials were liquid-like. It was observed that at temperatures
 345 greater than the gelling temperatures, the moduli of each formulation exhibited similar
 346 values, with a difference of 4, 8, 10 and 3% for 0, 1, 2 and 3% κC, respectively. As a
 347 result of the finding that the viscoelastic properties were no longer dependent on the
 348 temperature when the gelling point was exceeded, it is likely there would likely be no
 349 material benefit to printing at a higher temperature.

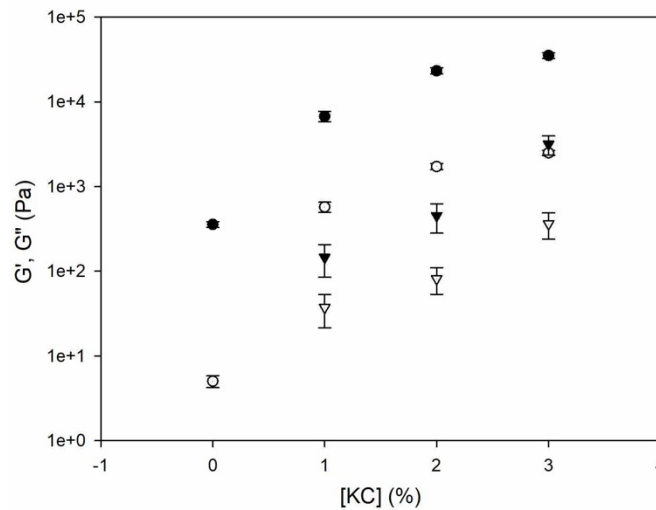
350

351 When the testing temperature was reduced below the gelling temperatures of each of
 352 the four formulations, G' and G'' became independent of frequency, indicating
 353 confirmation of the solid-like state of the material (Derkach et al., 2015). This result
 354 was also observed by del Carmen Núñez-Santiago and Tecante (2007) who
 355 investigated the evolution of moduli of 1% κC.

356

357 Figure 5 depicts the value of G' and G'' for all the four formulations taken from the
 358 frequency sweeps, at a value of 1 Hz and at temperatures of 20°C and 50°C. At all
 359 temperatures tested, as the concentration of κC was increased, the G' increased. This
 360 was the result of the synergistic effects of the gelatin and κC (Derkach et al., 2015).
 361 The hydrogen bonds formed with κC were stronger than those formed with just gelatin
 362 molecules. Costakis et al. (2016) determined that an increase in G' would allow better

363 shape retention post printing. The greater the value of the G' indicated higher gel
364 strength, which would enable the material to retain its shape following extrusion.
365



366
367
368

Figure 5. Frequency sweeps of 5% gelatin and different concentrations of κC at 20°C (○) and 50°C (◻), open symbols are the G'' , while closed symbols are the G' . ($n=3 \pm \text{SD}$).

369

370 3.3. Creation of an extrusion simulation

371 A simple simulation of the extrusion process was developed using a rotational
372 rheometer in order to determine the behaviour of the material during extrusion. The
373 simulation consisted of two parts: firstly, a viscosity curve was undertaken to mimic
374 the extrusion of the material using the average shear rate established previously;
375 secondly, small deformation rheology was employed to monitor the structuring of the
376 material on the plate post-printing.

377

378 The viscosity curves, at a shear rate of 100 s^{-1} , from a temperature of 60°C to 20°C,
379 of all four formulations is shown in Figure 6. There was a rapid increase in viscosity at
380 22°C, 34°C, 37°C and 42°C for 5% gelatin with 0, 1, 2 and 3% κC respectively. These
381 values were very similar to the gelling temperatures found previously using both the
382 μDSC and the rheometer, this increase in viscosity was therefore attributed to the
383 gelling of the material. The results obtained for the 5% gelatin are in agreement with
384 those obtained by Madhamathanalli and Bangalore (2014), who determined that at 25
385 °C the viscosity was 0.032 Pa.s, while the results for the 1% κC are similar to those
386 obtained by Gabriele et al. (2009).

387

388 It has been noted previously that the minimum material viscosity required to
389 successfully print was 0.03 Pa.s (Murphy and Atala, 2014). Only the formulations with
390 2 and 3% κC were above this minimum viscosity throughout the range of temperatures
391 tested. The viscosities of the formulations with 0 and 1 % κC were below this minimum
392 value of viscosity, until the temperatures exceed their gelling temperatures and the
393 materials started to gel. If these formulations were extruded at a temperature too far
394 above their gelling temperatures, the viscosity might be too low, resulting in material
395 which just flows out of the nozzle, particularly in cases where the surface tension is
396 not sufficiently great to prevent it (He et al., 2015).

397

398 Analysis of the recovery of the material was important in order to determine whether
399 the material would spread after extrusion and whether subsequent layers could be
400 printed onto it. The recovery graphs show how both the G' (figure 7 A) and G'' (figure
401 7 B) behaved following removal of the shear whilst at a constant temperature of 20 °C.
402 The graph only records results up to 200s as, within this timeframe, any additional
403 layers would be printed. As soon as the shear was removed all of the formulations
404 displayed an elastically dominant system. The time taken for the system to reach an
405 equilibrium, which meant that the system was a solid gel, was a function of κC
406 concentration. The curves were fit to an exponential growth equation, shown in
407 equation 3.

408

$$409 \quad y = y_0 + a(1 - e^{-bt}) \quad [3]$$

410

411 *Where y is G' , y_0 is the initial G' , a is the final growth, b is the rate of growth and t is*
412 *time.*

413

414 The maximum value of G' found for 3, 2, 1 and 0% κC was found to be 4, 2, 0.6 and
415 0.4 Pa respectively. Once these values had been obtained from each of the individual
416 curves, the recovery of the formulations with 3, 2 and 1% κC at 2 minutes was found
417 to be 75%, 73% and 67% of their maximum G' values respectively. The formulation
418 without the κC only recovered to 45% of its maximum G' value, indicating that the
419 recovery occurred a lot faster for the formulation with κC compared to the formulation
420 without, as a result of the strong interactions between the gelatin and κC molecules.

421

422 3.4. Determination of printability using the rheological data

423 Printability was evaluated by assessing the uniformity of the extrusion during the
424 printing process along with the accuracy and stability of the printed part (Lille et al.,
425 2017). The temperature control within the printing process was of utmost importance
426 due to the temperature dependence sol-gel transition of gelatin (Billiet et al., 2014). It
427 was found previously that at temperatures higher than the gelling temperature the
428 viscoelastic properties of the material were similar. However, there was a change in
429 the properties when the gelling temperature was reached. In order to determine how
430 much the viscoelastic properties affected the printability, 2D and 3D squares were
431 printed out in each material, at its gelling temperature and at a higher temperature.

432

433 Each of the printed squares were intended to measure 20mm x 20mm with a width of
434 1mm and the extrusion commenced in the bottom left corner. The 2D squares were
435 printed with 1 layer (height of 0.3 mm) and the 3D squares were printed using 4 layers
436 (height of 1.2 mm). By printing both 2D (Figure 8) and 3D (Figure 9) structures of all
437 the formulations, at both their gelling temperatures and a higher temperature, it was
438 possible to determine whether the materials were gelling fast enough to allow layers
439 to be built up.

440

441 In order to determine the accuracy of the resultant printed squares, the width and the
442 height of each square was measured. This analysis process was similar to that of
443 Derossi et al. (2017) who measured the heights and width of a fruit-based formulation
444 to determine if their printed snacks matched the design structure. The width of the
445 printed square was measured at the bottom right corner, after the first corner, whilst
446 the height was measured at the four corners and averaged. The level of spreading
447 was determined by the deviation from the intended values.

448

449 Table 2 shows the results of the measurement of the width of the 2D and 3D squares
450 printed at both the formulations gelling temperature ($T=T_{gel}$) and at the higher
451 temperature ($T>T_{gel}$) for all systems tested with the addition of κ C. Deviation was
452 calculated as the percentage difference between the desired value of 1 mm and the
453 experimental widths found. Neither the 2D nor the 3D squares extruded with 'gelatin
454 only' formulation exhibited a uniform width, therefore these results were not presented.

455 The 2D and 3D squares, obtained by the printing of the formulation with no κC ,
456 displayed poor resolution, broken lines and a large amount of spreading. Costakis et
457 al. (2016) determined that materials with a higher G' resulted in better shape retention.
458 The G' for the formulation without any κC was 0.7 kPa resulting in pools of material
459 being formed rather than a solid line. The spreading occurred as the gelation process
460 was not rapid enough to prevent the material from spreading (Wei et al., 2015).

461

462 Spreading of the extruded material also occurred when the formulation with 1% κC
463 was printed. The width of the 2D squares were at least 40% larger than desired at both
464 temperatures printed. The spreading was not only due to the long gelation time of this
465 material and the low G' (ca. 4.5 kPa), but also due to the material phase separating.
466 When subsequent layers were added, more spreading occurred, with a large
467 difference of width observed between the two temperatures used for printing. The
468 squares printed at a higher temperature showed greater levels of spreading (240%)
469 compared to the squares printed at the gelling temperature (150%). The squares
470 printed at a lower temperature reached their gelation temperature faster, which
471 reduced the spreading of the material.

472

473 The width of the 2D squares printed with the addition of 2% κC were observed to be
474 within 10% of the standard value at both temperatures tested. In this instance over
475 73% of the material's structuring was recovered within 200s and that, combined with
476 the high G' (ca. 23 kPa), ensured that spreading was inhibited due to the strong elastic
477 network within the system being created quickly as a result of the fast recovery time.
478 When the 4 layer high, 3D square was printed using the 2% κC formulation, the width
479 of the square spread ca. 70%. This outcome was the result of insufficient adhesion
480 between the subsequent layers, as the material gelled too quickly to bond to the
481 previous layer, resulting in the newly deposited layer sliding off the lower layer. The
482 width of this formulation was similar at both of the temperatures tested for this
483 formulation, again owing to the fast gelation time.

484

485 The width of the 2D square printed with the mixture containing 3% κC was within 10%,
486 when printed at a temperature higher than its gelling temperature. When this
487 formulation was printed at its gelling temperature, the width was found to be a lot wider.

488 In Figure 8D, it can be seen that the square printed at the gelling temperature (42°C)
489 did not produce a shape with solid lines. This was likely to be due to the material
490 gelling within the nozzle itself resulting in extrusion of a solid material. The same
491 broken lines could also be seen when a 3D square was printed at this temperature
492 (Figure 9D). The 2D shape obtained when printing at a higher temperature was within
493 10% of the printed width, due to the fast gelation time and high G' of this material. The
494 4 layer high 3D shapes, printed using the formulation of 3% κC displayed a well printed
495 square, close to the desired width.

496

497 Table 3 documents the heights of the 2D and 3D printed squares at the formulations
498 gelling temperature ($T=T_{gel}$) and at the higher temperature ($T>T_{gel}$). The deviation was
499 calculated as the percentage difference between the desired values of 0.3 mm for 1
500 layer and 1.2 mm for 4 layers and the determined experimental heights. For the
501 formulation without κC, both the 2D and 3D squares achieved a greater than desired
502 height at the lower temperature tested. During printing of these squares, it was
503 observed that the material was dragged along, leading to excess material forming
504 pools rather than lines and resulting in the higher than expected heights. It would
505 appear that some structuring was occurring within this system, but not fast enough to
506 prevent the pools from forming. The height of the 2D printed square, printed at the
507 higher temperature (40°C) was lower than was desired due to the material not
508 structuring in time, therefore not able to hold the shape together. The height of the 3D
509 printed square at the higher temperature was observed to be over 50% less than the
510 desired height. The higher printing temperature and slow elastic network formation led
511 to the gelatin acting like a viscoelastic liquid. A 3D network of polymers was not able
512 to form, resulting in spreading of the material as the lower structure was unable to
513 support the subsequent layers and therefore the desired height was not achieved.

514

515 The table illustrates that, despite the fact both spread beyond the desired width, there
516 was a height difference between the 1% κC 2D squares printed at the gelling
517 temperature and the higher temperatures. For the formulation with 1% κC, an elastic
518 network began to form at 35°C. Printing at a slightly higher temperature caused a
519 minimal delay in the formation of the network. This delay in time prior to network
520 development increased when the printing temperature was increased to 50°C. The

521 result of this time differential led to the square printed at the lower temperature
522 achieving a greater height as a result of the quicker formation of the network. Using
523 the same formulation, the printed height the 3D shapes achieved was about 80% less
524 than the desired height. Despite the fact that the width was affected by spreading of
525 the printed material some height was achieved. This indicates that the observed large
526 width discovered was likely due to the phase separation of the material.

527

528 For the formulation with 2% κ C, the same printed height was achieved for the 2D
529 squares when extruding at both temperatures. The fast gelation time of this material
530 ensured that the temperatures did not affect the mixture. However, at both
531 temperatures, when the 3D squares were printed the height was greater than desired
532 along with the width. This was caused by the lack of bonding between the layers
533 leading to material which did not slip off the lower layers gelling on top of the previous
534 layer, leading to the height of the squares being greater than desired.

535

536 The squares obtained from printing the 5% gelatin and 3% κ C mixture at its gelling
537 temperature were broken and ill defined. The height of the 2D shapes was similar to
538 the squares printed with the mixture printed with 2% κ C. However, the squares
539 themselves were dissimilar with the uneven printing of the former giving a false
540 impression of height. When printed at the higher temperature, the height of the 2D and
541 3D squares were identical to the heights achieved with the formulation of 5% gelatin
542 and 2% κ C. The fast gelation time of this material enabled the printed object to retain
543 the desired shape.

544

545 As the concentration of the κ C within the system was increased, the printability of the
546 system improved, with printed squares of the formulation of 5% gelatin and 3% κ C
547 producing squares closest to the desired shape.

548

549 4. Conclusions

550 This paper presents an assessment of the printability of 5% gelatin solutions with
551 additions of κ C in order to establish design rules for the printing of thermally gelling
552 hydrocolloids. It was found that in order to print well defined structures, the magnitude
553 of the G' needed to be greater than 2 kPa at the printing temperature and greater than

554 23 kPa at the temperature of the environment in which the object was being printed
555 (during these experiments the temperature of the room was set to 20°C). It was also
556 necessary for the formulation to recover at least 73% of its maximum G' within 200s
557 which facilitated the rapid formation of an elastic network necessary to prevent
558 spreading and achieve shape retention.

559

560 It was established that the printing temperature affected the printability of the different
561 formulations. The addition of κC resulted in an increase in the gelling temperature
562 which enabled greater control of the printing as compared to the formulation of just
563 gelatin alone, which gelled just above room temperature. The increased gelling
564 temperature provided a greater temperature differential when printing at room
565 temperature, allowing the material to solidify faster and create the desired shape. In
566 general, the objects printed with the different formulations at their gelling temperatures
567 achieved a more defined structure with less spreading of the material. The exception
568 was of the formulation of 5% gelatin and 3% κC printed at room temperature, which
569 displayed poor printed shapes. This was due to the magnitude of the G' being too
570 great at this temperature, ca. 6 kPa which led to structuring within the nozzle, resulting
571 in the formulation being extruded as solid-like and leading to broken lines. When this
572 formulation was printed at an increased temperature, good printability was achieved.

573

574 The influence of rheological and thermal transitions on the printability of
575 thermoreversible materials outlined above could be applied to 3D printing of various
576 other materials undergoing the same thermal gelation process which will be the focus
577 of subsequent studies.

578

579 [Acknowledgements](#)

580 This research was funded by the Engineering and Physical Sciences Research
581 Council ([EP/K030957/1](#)).

582

583 **References**

- 584 ANTONOV, Y. A. & GONÇALVES, M. 1999. Phase separation in aqueous gelatin-κ-
585 carrageenan systems. *Food Hydrocolloids*, 13, 517-524.
- 586 BILLIET, T., GEVAERT, E., DE SCHRYVER, T., CORNELISSEN, M. & DUBRUEL, P. 2014. The 3D
587 printing of gelatin methacrylamide cell-laden tissue-engineered constructs with high
588 cell viability. *Biomaterials*, 35, 49-62.

589 BOHIDAR, H. B. & JENA, S. S. 1993. Kinetics of sol–gel transition in thermoreversible gelation
590 of gelatin. *The Journal of Chemical Physics*, 98, 8970-8977.

591 COHEN, D. L., LIPTON, J. I., CUTLER, M., COULTER, D., VESCO, A. & LIPSON, H. Hydrocolloid
592 printing: a novel platform for customized food production. Solid Freeform
593 Fabrication Symposium (SFF'09), 2009.

594 COSTAKIS, W. J., RUESCHHOFF, L. M., DIAZ-CANO, A. I., YOUNGBLOOD, J. P. & TRICE, R. W.
595 2016. Additive manufacturing of boron carbide via continuous filament direct ink
596 writing of aqueous ceramic suspensions. *Journal of the European Ceramic Society*,
597 36, 3249-3256.

598 CRUMP, S. S. 1992. Apparatus and method for creating three-dimensional objects. Google
599 Patents.

600 DEL CARMEN NÚÑEZ-SANTIAGO, M. & TECANTE, A. 2007. Rheological and calorimetric study
601 of the sol–gel transition of κ -carrageenan. *Carbohydrate polymers*, 69, 763-773.

602 DERKACH, S. R., ILYIN, S. O., MAKLAKOVA, A. A., KULICHIKHIN, V. G. & MALKIN, A. Y. 2015.
603 The rheology of gelatin hydrogels modified by κ -carrageenan. *LWT-Food Science and*
604 *Technology*, 63, 612-619.

605 DEROSI, A., CAPORIZZI, R., AZZOLLINI, D. & SEVERINI, C. 2017. Application of 3D printing for
606 customized food. A case on the development of a fruit-based snack for children.
607 *Journal of Food Engineering*.

608 DIAZ, J. V., VAN BOMMEL, K., J.C. , NOORT, M., W-J. & HENKET, J. B., P. 2014. *Method for*
609 *the production of edible objects using sls and food products*. France patent
610 application WO2014193226A1.

611 DIAZ, J. V., VAN BOMMEL, K. J. C., NOORT, M. W.-J., HENKET, J. & BRIËR, P. 2016. Method
612 for the production of edible objects using sls and food products. Google Patents.

613 DJABOUROV, M., LEBLOND, J. & PAPON, P. 1988. Gelation of aqueous gelatin solutions. II.
614 Rheology of the sol-gel transition. *Journal de Physique*, 49, 333-343.

615 GABRIELE, A., SPYROPOULOS, F. & NORTON, I. T. 2009. Kinetic study of fluid gel formation
616 and viscoelastic response with kappa-carrageenan. *Food Hydrocolloids*, 23, 2054-
617 2061.

618 GODOI, F. C., PRAKASH, S. & BHANDARI, B. R. 2016. 3d printing technologies applied for
619 food design: Status and prospects. *Journal of Food Engineering*, 179, 44-54.

620 GÓMEZ-GUILLÉN, M. C., GIMÉNEZ, B., LÓPEZ-CABALLERO, M. E. & MONTERO, M. P. 2011.
621 Functional and bioactive properties of collagen and gelatin from alternative sources:
622 A review. *Food Hydrocolloids*, 25, 1813-1827.

623 HAO, L., MELLOR, S., SEAMAN, O., HENDERSON, J., SEWELL, N. & SLOAN, M. 2010. Material
624 characterisation and process development for chocolate additive layer
625 manufacturing. *Virtual and Physical Prototyping*, 5, 57-64.

626 HARRINGTON, J. C. & MORRIS, E. R. 2009. Conformational ordering and gelation of gelatin in
627 mixtures with soluble polysaccharides. *Food Hydrocolloids*, 23, 327-336.

628 HE, Y., QIU, J., FU, J., ZHANG, J., REN, Y. & LIU, A. 2015. Printing 3D microfluidic chips with a
629 3D sugar printer. *Microfluidics and Nanofluidics*, 19, 447-456.

630 IJIMA, M., HATAKEYAMA, T., TAKAHASHI, M. & HATAKEYAMA, H. 2007. Effect of thermal
631 history on kappa-carrageenan hydrogelation by differential scanning calorimetry.
632 *Thermochimica Acta*, 452, 53-58.

633 JOLY-DUHAMEL, C., HELLIO, D., AJDARI, A. & DJABOUROV, M. 2002. All Gelatin Networks: 2.
634 The Master Curve for Elasticity. *Langmuir*, 18, 7158-7166.

635 KRUTH, J. P., LEU, M. C. & NAKAGAWA, T. 1998. Progress in Additive Manufacturing and
636 Rapid Prototyping. *CIRP Annals - Manufacturing Technology*, 47, 525-540.

637 LI, H., LIU, S. & LIN, L. 2016. Rheological study on 3D printability of alginate hydrogel and
638 effect of graphene oxide. *2016*, 2.

639 LILLE, M., NURMELA, A., NORDLUND, E., METSÄ-KORTELAJINEN, S. & SOZER, N. 2017.
640 Applicability of protein and fiber-rich food materials in extrusion-based 3D printing.
641 *Journal of Food Engineering*.

642 LIU, Z., ZHANG, M., BHANDARI, B. & YANG, C. 2017. Impact of rheological properties of
643 mashed potatoes on 3D printing. *Journal of Food Engineering*.

644 MADHAMUTHANALLI, C. V. & BANGALORE, S. A. 2014. Rheological and physico-chemical
645 properties of gelatin extracted from the skin of a few species of freshwater carp.
646 *International journal of food science & technology*, 49, 1758-1764.

647 MANGIONE, M. R., GIACOMAZZA, D., BULONE, D., MARTORANA, V., CAVALLARO, G. & SAN
648 BIAGIO, P. L. 2005. K⁺ and Na⁺ effects on the gelation properties of κ-Carrageenan.
649 *Biophysical Chemistry*, 113, 129-135.

650 MICHON, C., CUVELIER, G., RELKIN, P. & LAUNAY, B. 1997. Influence of thermal history on
651 the stability of gelatin gels. *International Journal of Biological Macromolecules*, 20,
652 259-264.

653 MORRISON, N. A., CLARK, R. C., CHEN, Y. L., TALASHEK, T. & SWORN, G. 1999. Gelatin
654 alternatives for the food industry. In: NISHINARI, K. *Physical Chemistry and Industrial*
655 *Application of Gellan Gum*. Berlin, Heidelberg: Springer Berlin Heidelberg.

656 MURPHY, S. V. & ATALA, A. 2014. 3D bioprinting of tissues and organs. *Nature*
657 *biotechnology*, 32, 773-785.

658 PARKER, N. & POVEY, M. 2012. Ultrasonic study of the gelation of gelatin: phase diagram,
659 hysteresis and kinetics. *Food Hydrocolloids*, 26, 99-107.

660 REES, D. A. 1972. Polysaccharide gels. A molecular view *Chem. Ind.*, 630.

661 TAKAYANAGI, S., OHNO, T., OKAWA, Y., SHIBA, F., KOBAYASHI, H. & KAWAMURA, F. 2000.
662 Sol-gel transition of a mixture of gelatin and κ-carrageenan. *The Imaging Science*
663 *Journal*, 48, 193-198.

664 TOSH, S. M. & MARANGONI, A. G. 2004. Determination of the maximum gelation
665 temperature in gelatin gels. *Applied Physics Letters*, 84, 4242-4244.

666 VAN VLIET, T. 2013. *Rheology and fracture mechanics of foods*, CRC Press.

667 WANG, L., CAO, Y., ZHANG, K., FANG, Y., NISHINARI, K. & PHILLIPS, G. O. 2015. Hydrogen
668 bonding enhances the electrostatic complex coacervation between κ-carrageenan
669 and gelatin. *Colloids and Surfaces A: Physicochemical and Engineering Aspects*, 482,
670 604-610.

671 WEI, J., WANG, J., SU, S., WANG, S., QIU, J., ZHANG, Z., CHRISTOPHER, G., NING, F. & CONG,
672 W. 2015. 3D printing of an extremely tough hydrogel. *Rsc Advances*, 5, 81324-81329.

673 WOHLERS, T. & GORNET, T. 2012. History of additive manufacturing.

674 WONG, K. V. & HERNANDEZ, A. 2012. A Review of Additive Manufacturing. *ISRN Mechanical*
675 *Engineering*, 2012, 10.

676 YANG, F., ZHANG, M., BHANDARI, B. & LIU, Y. 2018. Investigation on lemon juice gel as food
677 material for 3D printing and optimization of printing parameters. *LWT-Food Science*
678 *and Technology*, 87, 67-76.

679
680

681 Table 1

Gelling temperature (°C)		
	Onset of exotherm	Cross-over temperature
5% gelatin	24 ± 0.4	22 ± 0.2
5% gelatin and 1% κC	36 ± 0.4	36 ± 1.3
5% gelatin and 2% κC	39 ± 0.01	42 ± 0.9
5% gelatin and 3% κC	42 ± 0.01	-

682

683

684 Table 2

		Concentration of κ C added (%)					
		1		2		3	
	No. of layers	Width (mm)	Deviation (%)	Width (mm)	Deviation (%)	Width (mm)	Deviation (%)
$T=T_{Gel}$	1	1.6 \pm 0.1 ^a	60	1.1 \pm 0.1 ^{ab}	10	1.6 \pm 0.5 ^b	60
	4	2.5 \pm 0.4 ^a	150	1.8 \pm 0.2	80	1.7 \pm 0.7 ^a	70
$T \gg T_{Gel}$	1	1.4 \pm 0.2 ^{ab}	40	1.1 \pm 0.05 ^a	10	1.1 \pm 0.1 ^b	10
	4	3.4 \pm 0.6 ^{ab}	240	1.7 \pm 0.2 ^a	70	1.4 \pm 0.2 ^b	40

685

686

		Concentration of κ C added (%)							
		0		1		2		3	
	No. of Layers	Height (mm)	Deviation (%)	Height (mm)	Deviation (%)	Height (mm)	Deviation (%)	Height (mm)	Deviation (%)
$T=T_{Gel}$	1	0.5 ± 0.08^{abc}	67	0.3 ± 0.09^{ad}	0	0.2 ± 0.08^b	- 33	0.2 ± 0.06^{cd}	- 33
	4	1.6 ± 0.1^{abc}	33	1.0 ± 0.2^{ad}	- 17	1.3 ± 0.2^{bde}	8	0.9 ± 0.05^{ce}	- 25
$T \gg T_{Gel}$	1	0.2 ± 0.1	- 33	0.2 ± 0.07	- 33	0.2 ± 0.07	- 33	0.2 ± 0.04	- 33
	4	0.5 ± 0.1^{abc}	- 58	0.9 ± 0.2^{ade}	- 25	1.4 ± 0.1^{bdf}	17	1.3 ± 0.1^{cef}	8